Bulgarian Chemical Communications, Volume 45, Number 4 (pp. 434–439) 2013

Preparation, structure and catalytic properties of $ZnFe_2O_4$

K. V. Koleva[1]*, N. I. Velinov[1], T. S. Tsoncheva[2],
I. G. Mitov[1], B. N. Kunev[1]

[1] *Institute of Catalysis, BAS, Sofia, 1113, Bulgaria*
[2] *Institute of Organic Chemistry with Centre of Phytochemistry, BAS, Sofia, 1113, Bulgaria*

Received February, 2013; Revised May, 2013

Zinc ferrite ($ZnFe_2O_4$) nanopowders were prepared by co-precipitation method from the corresponding nitrate precursors and thermal treating of the obtained precursor at different temperatures. X-ray diffraction and ^{57}Fe Mössbauer spectroscopy were used for the characterization of the obtained materials. The results of X-ray analysis confirm formation of nanocrystalline zinc ferrite phase with cubic structure and crystallite size 6–46 nm depending on the annealing temperature. The obtained ferrites were tested as catalysts in methanol decomposition to CO and hydrogen. The analyses of the samples after the catalytic test reveal a significant phase transformation of the ferrite phase by the influence of the reaction medium.

Key words: zinc ferrite, Mössbauer spectroscopy, methanol decomposition.

INTRODUCTION

The magnetic, dielectric and electrical behavior of the ferrite materials provides their large scale of applications, as semiconductors [1], pigments [2], magnetic resonance imaging [3], computer memory chips. Their catalytic properties have been tested in number of industrial process, such as oxidative dehydrogenation of hydrocarbons, decomposition of alcohols [4] and hydrogen peroxide, treatment of automobile-exhausted gases, phenol hydroxylation (oxidation), photocatalytic ozonation of dyes [5] and alkylation of hydrocarbons [6].

Recent studies concerned methanol as a potential source of hydrogen for fuel cells because of its relatively low temperature of decomposition to hydrogen, high energy density, safety handle, low cost and possibility of production from renewable sources as biomass [7–11].

The aim of present work is to study preparation of zinc ferrite nanopowders by co-precipitation method following by thermal treatment and to study the catalytic activity in methanol decomposition to CO and hydrogen. The changes in the phase composition of materials after the catalytic test were also in the focus of investigation. Mössbauer technique was used due to its high sensitivity to investigate the phase composition, magnetic behavior and iron ions emplacement of unit cell [12].

In our previous work the synthesis of $CuFe_2O_4$ [13, 14], $CoFe_2O_4$ [15, 16], $NiFe_2O_4$ [17] and mixed Ni-$ZnFe_2O_4$ ferrite materials [18] was reported. Methods of Spark Plasma Sintering, sol-gel, thermal and mechanochemical treatments [19, 20] have been applied successfully. The relationship between parameter of synthesis, phase composition, particle size, microstrain and catalytic behavior of ferrite materials has been discussed. Application of Cu, Ni, and Co based ferrites is well known, especially when these elements are substituted with Zn ions, which prefer the tetrahedral position in spinel lattice and has strong effect on the properties. It is well known that Zn content exerts important role on structure and properties of ferrites [21, 22]. In this work we demonstrate synthesis, structure and catalytic properties of pure zinc ferrite.

EXPERIMENTAL

Synthesis

Four samples of zinc-iron oxide powders were prepared by co-precipitation method. Water solution containing Zn- and Fe-ions was prepared of stoichiometric amount of nitrate salts [$Zn(NO_3)_2.6H_2O$;

* To whom all correspondence should be sent:
E-mail: kremena_vassileva@abv.bg

$Fe(NO_3)_3.9H_2O$]. As a precipitation agent was used 1M Na_2CO_3 and pH was kept of 9. The obtained precipitates were washed with distilled water and dried at room temperature to form precursor powders. The heat treatment of precursors was conducted in air at 573 K, 673 K, 773 K, 973 K for four hours to obtain ferrite samples.

Characterisation

The powder XRD patterns were recorded by a TUR M62 diffractometer with Co Kα radiation. The observed patterns were cross-matched with those in the JCPDS database [23]. The average crystallites size (D), the degree of microstrain (e) and the lattice parameters (a) of the studied ferrites were determined from the experimental XRD profiles by using the PowderCell-2.4 software [24]. The instrumental broadening of diffraction peaks is equal to 0.020° Bragg angle. It was determined by Al standard and was excluded at calculation of crystallites size and the degree of microstrain. The Mössbauer spectra were obtained at room temperature (RT) with a Wissel (Wissenschaftliche Elektronik GmbH, Germany) electromechanical spectrometer working in a constant acceleration mode. $^{57}Co/Rh$ (activity ≅50 Ci) source and α-Fe standard were used. The experimentally obtained spectra were fitted using CONFIT2000 software [25]. The parameters of hyperfine interaction such as isomer shift (IS), quadrupole splitting (QS), effective internal magnetic field (Heff), line widths (FWHM), and relative weight (G) of the partial components in the spectra were determined.

Catalytic test

Methanol decomposition experiments were carried out in a flow reactor using argon as a carrier gas, at methanol partial pressure of 1.57 kPa and WHSV of 1.5 h^{-1}. On-line gas chromatographic analysis were performed on HP 5980 on PLOT Q column, with simultaneous using of detector of thermo conductivity and flame ionization detector and an absolute calibration method.

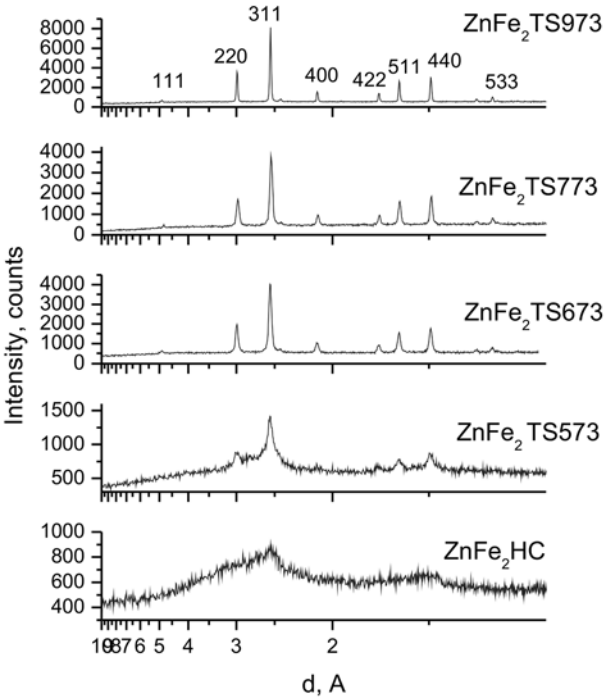

Fig. 1. X-ray diffraction patterns of synthesized samples

RESULTS AND DISCUSSION

XRD patterns of the precursor powder and thermally synthesized samples are presented in Fig. 1. Beginning of crystallization process was observed at temperature as low as 573K. The diffractograms of samples treated at higher temperatures show well defined reflexes corresponding to cubic spinel phase of zinc ferrite with lattice parameter a= 8.43–8.44 Å. Microstrain degree and average crystallite size of zinc ferrite powders was calculated using Williamson–Hall equation and presented in Table 1.

Table 1. Average crystallite size (D), degree of microstrain (e) and lattice parameters (a) determined from experimental XRD profiles

Sample	Phase	D, nm	$e.10^3$, a.u	a, A
$ZnFe_2TS573$	Fd3m(227) – cubic	5.89	7.894	8.43
$ZnFe_2TS673$	Fd3m(227) – cubic	19.09	1.228	8.43
$ZnFe_2TS773$	Fd3m(227) – cubic	19.08	1.323	8.44
$ZnFe_2TS973$	Fd3m(227) – cubic	45.84	1.187	8.43

Increasing of crystallite size from 6 to 46 nm and narrowing the width of the peaks with increasing of temperature in the range of 573–973 K can be explain with effect of sintering.

The room temperature Mössbauer spectroscopy is presented in Fig. 2. The Mössbauer spectra are consisted of well-defined doublet, typical of paramagnetic state of materials. The fitting parameters of Mössbauer spectra are presented in Table 2. Parameters of all spectra correspond to octahedral coordinated Fe^{3+} ions. Increasing of the value of superfine quadrupole splitting after treatment at 573 K could be assigned to additional deformation of octahedral Fe^{3+}, as a result of precursor decomposition. Further increasing of treatment temperature leads to decrease of QS to reach values typical for well crystallized zinc ferrite.

Temperature dependencies of conversion and CO selectivity in methanol decomposition of synthesized materials are presented in Figure 3. All ferrites started to decompose the methanol above 500 K and the conversion was about 90–95% at 600 K. Carbon monoxide was formed with 50–70% selectivity and methane and CO_2 were also registered as by products. A well defined tendency for the catalytic activity decrease with the increase of the temperature of ferrite synthesis was observed.

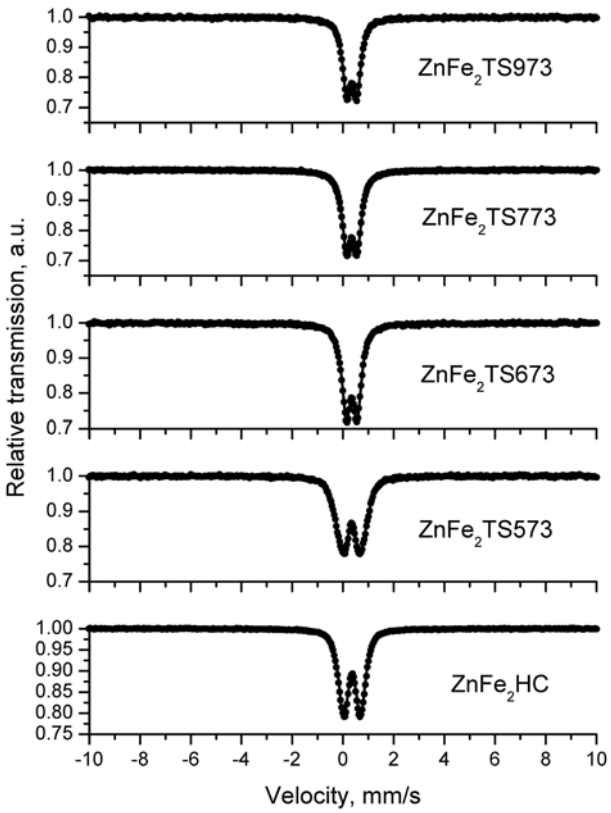

Fig. 2. Mössbauer spectra of synthesized samples

Table 2. Parameters of Mössbauer spectra of the investigated samples

Sample	Components	IS mm/s	QS mm/s	$H_{eff,}$ T	FWHM mm/s	G,%
$ZnFe_2HC$	Db	0.36	0.67	–	0.44	100
$ZnFe_2TS573$	Db	0.35	0.72	–	0.56	100
$ZnFe_2TS673$	Db	0.35	0.44	–	0.40	100
$ZnFe_2TS773$	Db	0.35	0.42	–	0.41	100
$ZnFe_2TS973$	Db	0.35	0.40	–	0.38	100

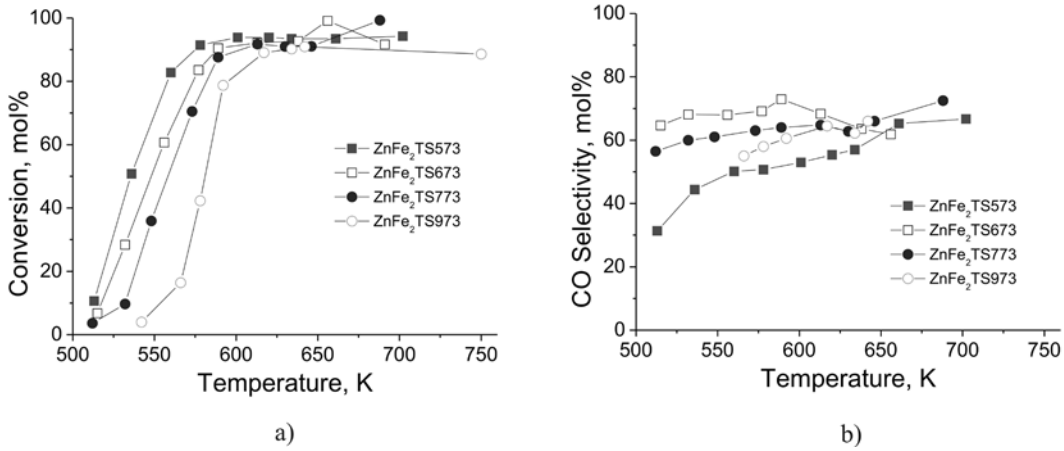

Fig. 3. Methanol conversion (A) and CO selectivity (B) vs. temperature of investigated ferrite materials

The phase transformation of used materials after catalytic test has been obtained by Mössbauer measurement (Fig. 4). The Mössbauer spectra of used sample $ZnFe_2O_4$ TS-973 was well fitted with two sextets of Zn-substituted magnetite, one sextets of non-stoichiometric carbide (Fe_xC_x), α-Fe and doublet of wuestite (FeO). Spectra of the other materials consist of sextets with parameters corresponding to $Zn_xFe_{3-x}O_4$ and Fe_5C_2 phases and zinc ferrite with relative part of 4–13% was also registered (Table 3). The Zn-substituted magnetite could be presented with the formula $(Zn^{2+}_xFe^{3+}_{1-x})_{tetra}[Fe^{3+}_{1+x}Fe^{2+}_{1+x}]_{octa}O_4$, as the spinel structure is preserved in the range $0 \leq x \leq 1$. Mössbauer spectrum of magnetite (Fe_3O_4) i.e. x = 0 consist of two Zeeman sextets. One of them is due to tetrahedral Fe^{3+} ions and other is due to octahedral Fe^{3+} and Fe^{2+} ions rendered indistinguishable by electron hopping at a frequency faster than that of the Larmor precession of the iron nucleus in the hyperfine field [26]. Therefore, the ratio of relative weight of two sextet components of unsubstituted magnetite should be 1:2 for Fe_{tetra}:Fe_{octa}, assuming of equal Mössbauer–Lamb factors for the different iron sites. The ratio of fitted relative weight of Sx1

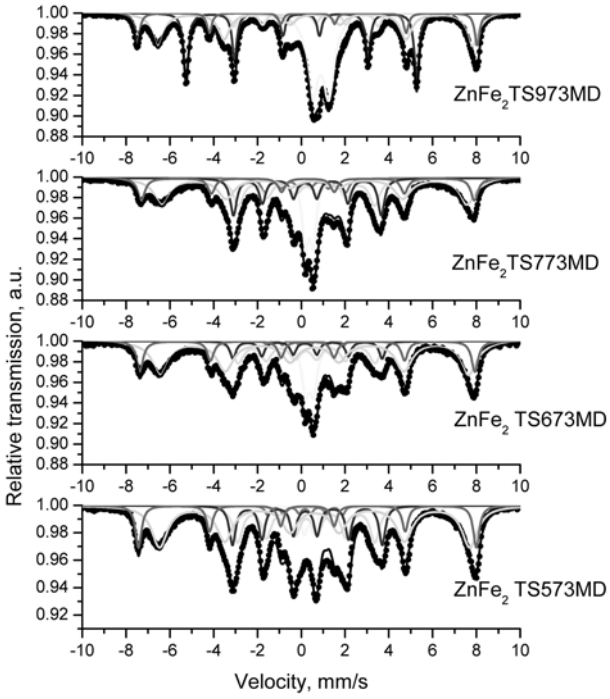

Fig. 4. Mössbauer spectra of samples after catalytic test

Table 3. Parameters of Mössbauer spectra of the investigated samples after catalytic test

Sample	Components		IS, mm/s	QS, mm/s	Heff, T	FWHM, mm/s	G, %
$ZnFe_2$TS573-MD	$Zn_xFe_{3-x}O_4$ (x = 0.30)	Sx1	0.28	0.00	47.9	0.33	14
		Sx2	0.60	0.01	44.0	0.87	40
	Fe_5C_2	Sx3	0.23	0.09	21.3	0.34	16
		Sx4	0.23	0.00	19.4	0.52	22
		Sx5	0.17	0.01	10.6	0.28	3
	$ZnFe_2O_4$	Db	0.35	0.44	–	–	4
$ZnFe_2$TS673-MD	$Zn_xFe_{3-x}O_4$ (x= 0.36)	Sx1	0.28	–0.01	47.5	0.36	14
		Sx2	0.60	0.00	43.7	0.89	44
	Fe_5C_2	Sx3	0.22	0.11	21.2	0.32	8
		Sx4	0.22	0.04	19.4	0.60	20
		Sx5	0.17	0.02	10.1	0.15	1
	$ZnFe_2O_4$	Db	0.37	0.37	–	–	12
$ZnFe_2$TS773-MD	$Zn_xFe_{3-x}O_4$ (x = 0.20)	Sx1	0.30	0.00	47.2	0.39	12
		Sx2	0.59	0.00	43.2	0.88	30
	Fe_5C_2	Sx3	0.30	0.10	21.0	0.36	18
		Sx4	0.23	0.00	19.3	0.57	20
		Sx5	0.17	0.02	11.5	0.38	7
	$ZnFe_2O_4$	Db	0.36	0.35	–	–	13
$ZnFe_2$TS973-MD	$Zn_xFe_{3-x}O_4$ (x = 0.21)	Sx1	0.28	–0.02	48.2	0.26	11
		Sx2	0.63	0.00	44.6	0.63	28
	α-Fe	Sx3	0.00	0.01	32.7	0.27	23
	Fe_xC_x	Sx4	0.17	0.07	20.4	0.36	8
	FeO	Db	0.88	0.73	–	0.60	30

and Sx2 of samples after catalytic reaction (Table 3) is higher than 1:2. This is due to presence of Zn-ions substitution of Fe^{3+} in tetrahedral position of magnetite lattice. The degree of Zn substitution x can be easily calculated by formula: x = 1 – 2A/B, where A and B are relative weight of Sx1 and Sx2, respectively.

CONCLUSION

Nanocrystalline zinc ferrites with cubic structure and particle size 6–45 nm were successfully synthesized by co-precipitation method. All investigated ferrite materials revealed good catalytic activity and selectivity to CO in methanol decomposition and it can be denoted that the final composition of the catalytic materials was formed in the reaction medium.

Acknowledgement: *Sponsorship by the Bulgarian National Science Fund at the Ministry of Education, Youth and Science under Project FFNNIPO_12_00182/2012 is gratefully acknowledged.*

REFERENCES

1. A. S. Kindyak, *Materials Letters*, **39**, 12 (1999).
2. A. C. F. M. Costa, A. M. D. Leite, H.S. Ferreira, R. H. G. A. Kiminami, S. Cava, L. Gama, *J. Europ. Ceram. Soc.*, **28**, 2033 (2008).
3. H. Wu, G. Liu, X. Wang, J. Zhang, Y. Chen, J. Shi, H. Yang, H. Hu, S.Yang , *Acta Biomaterialia*, **7**, 3496 (2011).
4. N. I. Maksimova, O. P. Krivoruchko, *Chemical Engineering Science*, **54**, 4351 (1999).
5. N. M. Mahmoodi, *Desalination*, **279**, 332 (2011).
6. P. Siwach, S. Singh, R. K. Gupta, *Catalysis Communications*, 1**0**, 1577 (2009).
7. J. Christopher Brown, Erdogan Gulari, *Catalysis Communications*, **5**, 431 (2004*).*
8. C.-C. Chang, C.-T. Chang, S.-J. Chiang, B.-J. Liaw, Y.-Z. Chen, *Intern. J. Hydrogen Energy*, **35**, 7675 (2010).
9. R. A. Dagle, A. Platon, D. R. Palo, A. K. Datye, J. M. Vohs, Y. Wang, *Applied Catalysis A: General*, **342**, 63 (2008).
10. T. Tsoncheva, J. Roggenbuck, M. Tiemann, L. Ivanova, D. Paneva, I. Mitov, C. Minchev, *Microporous and Mesoporous materials*, **110**, 339 (2008).
11. T. Tsoncheva, J. Rosenholm, C. V. Teixeira, M. Dimitrov, M. Linden, C. Minchev, *Microporous and Mesoporous Materials*, **89**, 209 (2006).
12. S. Kamali-M., T. Ericsson, R. Wäppling, *Thin Solid Films*, **515**, 721 (2006).
13. T. Tsoncheva, E. Manova, N. Velinov, D. Paneva, M. Popova, B. Kunev, K. Tenchev. I. Mitov, *Catalysis Communications*, **12**, 105 (2010).
14. E. Manova, .Tsoncheva, D. Paneva, M. Popova, N. Velinov, B. Kunev, K. Tenchev, I. Mitov, *Journal of Solid State Chemistry*, **184**, 1153 (2011).
15. E. Manova, T. Tsoncheva, C. Estournes, D. Paneva, K. Tenchev, I. Mitov, L. Petrov, *Applied Catalysis A: General*, **300**, 170 (2006).
16. E. Manova, T. Tsoncheva, D. Paneva, , I. Mitov, K. Tenchev, L. Petrov, *Applied Catalysis A: General*, **277**, 119 (2004).
17. E. Manova, T. Tsoncheva, D. Paneva, J. L. Rehspringer, K. Tenchev, I. Mitov, L. Petrov, *Applied Catalysis A: General*, **317**, 34 (2007).
18. N. Velinov, E. Manova, T. Tsoncheva, C. Estournes, D. Paneva, K. Tenchev, V. Petkova, K. Koleva, B. Kunev, I. Mitov, *Solid State Sciences*, **14**, 1092 (2012).
19. X. Wang, O. Tanaike, M. Kodama, H. Hatori, *Journal of Power Sources*, **168**, 282 (2007).
20. G. A. El-Shobaky, A .M. Turky, N. Y. Mostafa, S. K. Mohamed, *Journal of Alloys and Compounds*, **493**, 415 (2010).
21. M. Ajmal, A. Maqsood, *Materials Science and Engineering B*, **139**, 164 (2007).
22. K. B. Modi, P. V. Tanna, S. S. Laghate, H. H. Joshi, *Journal Of Materials Science Letters* **19**, 1111 (2000).
23. International Centre for Diffraction Data, Alphabetical Indexes, Pannsylvania 19073–3273, sets 1–44 (1998).
24. W. Kraus, G. Nolze, PowderCell for Windows, Federal Institute for Materials Research and Testing, Berlin, (2000).
25. T. Žák, Y. Jirásková, CONFIT: Mössbauer spectra fitting program, *Surface and Interface Analysis*, **38**, 710 (2006).
26. D. C. Dobson, J. W. Linnet, M. M. Rahman, *J. Phys. Chem. Solids*, **31**, 2727 (1970).

СИНТЕЗ, СТРУКТУРА И КАТАЛИТИЧНИ СВОЙСТВА НА $ZnFe_2O_4$

К. В. Колева[1]*, Н. И. Велинов[1], Т. С. Цончева[2],
И. Г. Митов[1], Б. Н. Кунев[1]

[1] *Институт по Катализ, БАН, София, 1113, България*
[2] *Институт по Органична химия с център по Фитохимия, София, 1113, България*

Постъпила февруари, 2013 г.; приета май, 2013 г.

(Резюме)

Наноразмерен цинков ферит ($ZnFe_2O_4$) беше синтезиран по метод на съутаяване от съответните метални соли с последващо термично третиране на получените предходници при различни температури. Всички образци бяха охарактеризирани с Рентгенов дифракционен анализ и Мьосбауерова спектроскопия. Резултатите получени от Рентгенофазовия анализ показват формиране на добре изкристализирала феритна фаза с кубична структура и размери на кристалитите в граници 6–46 nm, в зависимост от прилаганата температура на синтез. Получените след термична обработка феритни материали бяха изследвани в реакция на разлагане на метанол до CO и водород. Проведените анализи на образците след каталитичния тест показват значителна фазова трансформация на феритната фаза под влияние на реакционната среда.